


## ORIGINAL RESEARCH

# Voltage regulation in low voltage distribution networks with unbalanced penetrations of photovoltaics and battery storage systems

 Alexander Micallef  | Cyril Spiteri-Staines | John Licari

Department of Electrical Engineering, University of Malta, MSIDA, Malta

**Correspondence**
 Alexander Micallef, Department of Electrical Engineering, University of Malta, Room 421, Engineering Building, MSIDA 2080, Malta.  
Email: alexander.micallef@um.edu.mt
**Funding information**

Energy and Water Agency under the National Strategy for Research and Innovation in Energy and Water, Grant/Award Number: ESTELLE EWA 110/20/2/001-C

**Abstract**

Grid integration constraints are limiting the deployment potential of renewable energy sources in Malta. Large penetrations of photovoltaics in the low voltage (LV) distribution network pose a significant risk to grid stability due to their inherent intermittency and are known to cause overvoltages and reverse power flows. The authors evaluate how self-consumption strategies with distributed battery energy storage systems can contribute to the voltage regulation in LV networks and the reduction of reverse power flows. The batteries are controlled to absorb the reverse power flow at the dwellings' point of common coupling, before this is injected into the LV network. Simulations show that uncoordinated strategies are not suitable to address the distribution network challenges during reverse power flows and evening peak demands. On the other hand, self-consumption coordinated by a time-varying feed-in tariff (FiT) can provide higher profitability to the prosumers while providing added benefits to the utility. The net-billing profitability for the prosumers in a self-consumption scenario with time-varying FiT is transformed from the downward trend of the uncoordinated scenario to an upward trend against the increasing values of storage capacity.

**KEYWORDS**

demand side management, energy demand, EVs, power system simulation, storage

## 1 | INTRODUCTION

Malta has reached a renewable energy source (RES) share of 10.7% of the gross final energy consumption in 2020 [1]. With an 11.5% RES share set for 2030, photovoltaic (PV) generation is expected to remain Malta's highest RES contributor. In May 2022, the domestic sector accounted for 93.6% of the total number of PV installations with a peak average installed capacity of 3.2 kWp [2]. However, grid integration constraints are limiting the potential of RES deployment in Malta. Large penetrations of PVs pose a significant risk to grid stability due to their inherent intermittency. The wide-scale integration of residential PVs in the low-voltage (LV) distribution network are also known to cause (1) overvoltages; (2) reverse power flows (that could lead to thermal overloading); and (3) unbalanced PV integration across phases. These three challenges

reduce the effectiveness of conventional voltage regulation measures such as off-load/on-load tap changers and reactive power compensation.

Voltage rise/drop in radial LV distribution feeders with PVs is well known and documented in literature. The integration of battery energy storage systems (BESSs) is considered as one of the main solutions that enables high penetrations of RES in modern distribution networks. The readers are directed towards [3] for a comprehensive review of BESS integration in distribution networks. In this study, attention was given to self-consumption strategies aimed at behind-the-metre BESSs, limiting the reverse power flow, reducing the peak demand and over/undervoltage mitigation together with benefits to the prosumers (i.e., consumers with residential PV systems). Martin et al. [4] developed a generator dispatch model to increase the level of self-consumption of up

This is an open access article under the terms of the [Creative Commons Attribution](https://creativecommons.org/licenses/by/4.0/) License, which permits use, distribution and reproduction in any medium, provided the original work is properly cited.

© 2024 The Authors. *IET Smart Grid* published by John Wiley & Sons Ltd on behalf of The Institution of Engineering and Technology.

to 30% of the residential customers (having PV and BESS) in a Spanish network. The authors determined that although there was a significant reduction in the total energy used during the evening peak period, the impact on the peak demand was far less significant because the energy available in the BESS after daytime PV charging did not last long enough to completely offset the high evening loads. Similar findings were reported in Ref. [5], where the peak demand was reduced by only 5.7% for a cluster of households in the Netherlands. The modelled BESSs were sized to maximise the net present value (NPV) for each household under their existing retail tariffs resulting in an average of 3.4 kWh BESS capacity. This capacity was too small to have a large impact on the customers' demand during peaks. Another study by Martinez et al. [6] determined that a residential BESS sizing strategy for a standard IEEE 33-node test system that optimises the BESS NPV can lead to peak demand reductions of 31%. Ordóñez et al. [7] carried out a study on the profitability of self-consumption by residential prosumers in Ecuador and Spain under net-metering and net-billing schemes. In both countries, the best profitability was determined for prosumers with a high energy demand (annual consumption above 8000 kWh). However, the lower tariffs for imports and high retail electricity prices in Spain enable the average consumer to reach grid parity and make a profit. The authors in Ref. [8] consider a standard distribution feeder model with typical Australian LV feeder characteristics. The simulation study showed that the unbalanced integration of PV and BESSs can cause the network voltage to exceed the 2% voltage unbalance factor limit. El-Batawy and Morsi in Ref. [9] proposed a transactive energy framework in which the prosumers compete among each other through a dynamic Bertrand game to maximise their payoffs. The framework was tested in an IEEE 123-bus distribution feeder with three North American residential dwelling types. Simulation results have shown that prosumers may increase their daily profits by participating in the energy market by up to 224%.

In Ref. [10], the authors evaluated five tariff systems on the optimum size and operation of hybrid PV-battery systems in the Swiss LV networks. Two of the tariffs aimed to encourage self-consumption of PV energy, while another was a variable rate tariff and another two were hybrid tariffs with dual billing periods. These five tariffs were contrasted with two existing reference tariffs employed by the distribution system operator (DSO). Results showed that traditional volumetric tariffs yield comparable results to the two reference tariffs (flat and double tariff), offering no additional advantages in terms of the adoption and operation of PV-integrated battery systems. The authors in Ref. [11] proposed a data-driven approach that uses real-time hourly electricity consumption data from smart metres across Spain. This method enables a more comprehensive analysis compared to conventional yearly averages and takes into account the country's diverse demographics. The authors also assess the impact of different surplus compensation policies on the economic feasibility of rooftop PV installations in the Tarragona province (Spain). Day-ahead dynamic pricing strategies based on time-varying feed-in tariffs (FiTs), net metering, and net purchase/sale were evaluated in Ref. [12],

aimed at maximising consumer profits. The results show that the profitability of day-ahead dynamic pricing varies under each of the metering mechanisms. However, a probabilistic strategy was evaluated in this case that is highly sensitive to the input parameters and may not adapt well to real-time conditions. The authors in Ref. [13] proposed a hybrid tariff system that combines time-of-use pricing with location-based signals, with the goal of equitably distributing infrastructure expenses among users of the network. The authors show that time-of-use pricing is for the distribution network operators since peak hour electricity demands are the primary drivers for network reinforcements, while time-of-use signalling aids in optimising the utilisation of the network.

Other works have recently considered the use of centralised/decentralised strategies for the coordination of BESS in LV networks to provide over/undervoltage mitigation measures [14–21]. Two common limitations of these strategies are (1) the additional information and communications technology (ICT) infrastructure with bidirectional communication required to implement the algorithms; and (2) consumer awareness required on the provision of these services. In addition, strategies based on centralised/decentralised control of the BESSs introduce uncertainties in the consumer profitability as the BESS operation is dependent on the network conditions. In Refs. [14, 15], the authors propose a coordinated consensus-based strategy that controls the operation of the BESSs to regulate the feeder voltage. However, the strategy was tested for only small feeders of 6 and 7 buses respectively, with the consumers presenting identical PV and load profiles. Hashemi and Østergaard proposed a control approach in Ref. [16] that is based on the voltage sensitivity analysis to avoid overvoltages by determining dynamic set points for the BESSs. Simulations were performed on a balanced three phase feeder, and all consumers were assumed to have the same installed PV capacity and generation profiles. The authors in Ref. [17] proposed a coordinated control strategy for multiple BESSs based on voltage sensitivity analysis and a battery ageing model. The performance of this strategy was compared with an uncoordinated strategy for a real U.K. low voltage feeder with 106 consumers, out of which 42 have PV systems. However, 3 kW PV systems were assumed for this site, and storage units were placed using genetic algorithms rather than considering the possibility that each prosumer has the possibility/incentive to install a BESS. In Ref. [18], the authors proposed a receding horizon approach through model predictive control for the operation of two community scale BESSs in a balanced Italian LV network. The operation of the BESSs is determined from forecasts of demand and generation to counteract possible over/undervoltages in the network. Deeba et al in Ref. [19] propose a centralised control strategy through optimisation methods to support the operation of distribution networks. The control strategy enables to provide prosumers the ability to arbitrage while also enabling the provision of ancillary services. However, the control strategy was only tested on a 4.16 kV IEEE-13 distribution network that did not have distributed PV and BESSs. Procopiou et al. in Ref. [20] proposed an adaptive decentralised control strategy for residential-

scale BESSs to mitigate issues from overvoltages with a minimal effect on the consumers. The analysis was performed on a real Australian MV feeder with LV consumer data obtained from smart metres. However, the BESS control strategy is based on clear-sky irradiance values that introduce additional uncertainties in both the voltage regulation operation and the consumer profitability. Wang et al. in Ref. [21] propose deep reinforcement learning-based scheduling for BESSs to mitigate voltage deviations in unbalanced LV distribution networks. Simulations were performed on a customised 6-bus system and a modified IEEE 34-bus system. The performance of optimisation-based algorithms is heavily limited by the accuracy of forecasted PV generation and consumer electricity demand which reduces the practicality of these systems. In addition, modelling of unbalanced multi-phase LV distribution networks under dynamic conditions results in significant additional complexity.

This paper compares the effectiveness of uncoordinated and coordinated self-consumption strategies for voltage regulation purposes using the residential-scale BESSs. The first strategy models the present Maltese scenario based on real-time residential PV generation data and a correctly sized residential battery storage based on self-consumption with no coordination among the storage units. The second strategy consists of the development of a dedicated tariff system used for coordinated self-consumption using the behind-the metre BESSs. The aim of this coordinated control is aimed to benefit both the consumer and the utility. The research work carries out a direct comparison of the coordinated and uncoordinated scenarios. This shall be used to allow policy makers to determine the optimal way to implement residential battery storage systems and the tariff system that is beneficial to both consumers and the electrical utility. The authors explain and show the steps and analysis required to determine the dynamic FiT values based on the following criteria:

- High FiT during peak demand (encourages use of charged BESS home systems) aimed at reduction of the utility peak demand.
- Low FiT during periods of high PV generation (encourages charging of BESS) aimed at reduction of the reverse peak power flow.

In Malta, the majority of households have smart metres which record data at 15 or 30 min intervals. This shows that the households are already technology-ready for the implementation of time-varying tariffs as this study is proposing. The data for the real-time PV generation and load profiles from such metres was used for the analysis, and the results of which are presented in the paper. The analysis looked out at the results achieved when using the standard self-consumption for residential-scale BESS against those obtained using an optimal time-varying tariff-based system according to the time of use. The determination of the optimal dynamic FiT is aimed to mitigate voltage issues experienced by the consumers by reduction of the magnitude of the reverse power flow during peak PV generation and also the reduction of the evening peak

demand. As the number of residential-scale PV systems is expected to increase in Malta, it is critical to understand how the behaviour of BESSs effects the power quality of LV networks with the unbalanced penetration of PV systems. In this context, the main contributions of this paper are as follows:

- Initially, the occurrence of over/undervoltages in the Maltese LV distribution network due to the present PV penetrations is evaluated. Notably, there are no other studies within literature that address the specific case of the Maltese islands. This analysis relies on real data obtained from smart metres to show the expected voltage variations within the local distribution network considered in this work.
- In this study, coordinated and uncoordinated self-consumption strategies for over/undervoltage mitigation were designed, modelled and simulated. The uncoordinated strategy consists of a load-following modality that integrates key BESS constraints. A coordinated strategy based on time-varying FiT was proposed that also takes into consideration key BESS constraints. The over/undervoltage mitigation potential of present Maltese self-consumption strategies for behind-the-metre BESSs was simulated through modelling and simulation of a real-world application. Residential electricity consumption and generation profiles were obtained from smart metres (60 prosumers with PV only and 146 consumers without a PV or a BESS) to enhance the practicality and relevance of the study. The impact of voltage issues experienced by consumers through reductions in the magnitude of the reverse power flow during peak PV generation and a decrease in evening peak demand achieved through both strategies were then compared.
- Time-varying FiTs lead to an effectively simple implementation of energy arbitrage for prosumers in the LV network. As overvoltage issues are mainly due to high solar PV generation, the charging schedule of BESSs can be determined by the time-varying FiT bands during peak generation hours. The BESSs limit the reverse power flow and mitigate the voltage deviations until these reach the maximum State of Charge (SoC) limit. Similarly, undervoltage issues were mainly due to the evening peak demand. The BESS discharging schedule can also be determined by the time-varying bands. In both scenarios, some seasonality is expected that was averaged out by designing the FiT time bands over the average annual net demand.
- Although existing literature has focused on the charging/discharging schedules of BESSs using centralised and decentralised strategies, most of these studies were only limited to balanced networks or generated network architectures. In contrast, this paper presents results that are grounded in real network data, and combines both single phase and three phase consumers.

This paper is organised as follows. Section 2 presents an overview of the methodology used in this study. Section 3 describes the model of a substation in the Maltese LV distribution network. Section 4 describes the coordinated and

uncoordinated distributed behind-the-metre BESS strategies that are considered in this study. Section 5 summarises and discusses the simulation results, while the conclusion is presented in Section 6.

## 2 | METHODOLOGY

The modelling, simulation and analysis summarised in this paper were constrained to a secondary substation in the Maltese LV distribution network that has 182 nodes, with 192 single-phase consumers and 14 three-phase consumers connected to it. The consumers are divided on 5 feeders connected to the secondary LV side of an 11/0.4 kV and 250 kVA transformer. Net-demand profiles for each of the single-phase and three-phase consumers were obtained from the local DSO in the form of a single spreadsheet for a one-year period from 01 May 2020 to 31 April 2021 with a 15-min time resolution. The installed PV capacity and the generation profiles for each of the residential-scale PV systems were also obtained in the same format. Technical data on each of the cable/overhead lines were also included in the model that consists of the cable type per section, section lengths, and electrical parameters per unit length (resistance, inductance, and line-to-line capacitance). The PV generation sources were also modelled accurately, making use of the power-production profile data of each home's PV system. Figure 1 shows the LV line diagram for all the homes connected to the substation, and Table 1 shows the number of PV systems per phase per feeder. From this table, it can be observed that the PV production is not balanced between the different phases and feeders.

In this study, the distributed BESSs were considered to be deployed with every PV systems present in the network. Optimal battery sizing and placement strategies are trivial to the study being performed in this paper as the intention is to show the effect of coordinated and uncoordinated BESSs on the voltage profiles of the LV network. The effect on the voltage profile will still be present whether the battery is optimally sized or not and depending on how the BESS is operated. However, different battery sizes have been considered to show how the voltage profiles at the respective nodes are affected. Each BESS is controlled to absorb the reverse power flow at the dwellings' point of common coupling (PCC), before this is injected into the LV network. The following assumptions were considered for the simulations of the BESSs:

- The battery self-discharge rate was considered negligible.
- Round-trip energy efficiency is of 85% (includes the battery and power electronic converter efficiencies).
- The efficiency of the power electronic converter does not vary with the output power from the BESS.
- The SoC varies between 15% and 100%.
- The BESS charging and discharging currents are limited to a rate of 1C.
- The BESS is assumed to be discharged at the start of the simulation (initial SoC of 15% at 00:00 AM).
- Other battery-specific characteristics were not considered.

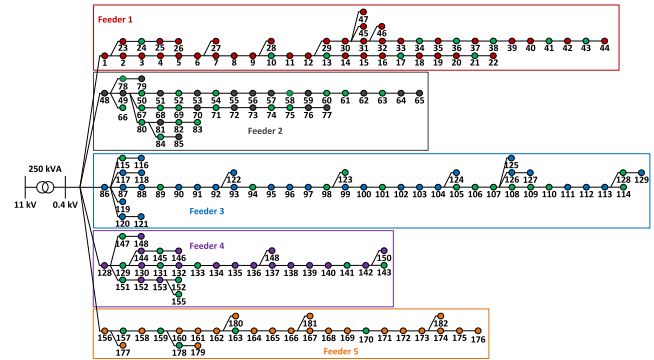


**FIGURE 1** Simplified line diagram of the low voltage network at the secondary substation. Feeder nodes are colour coded for ease of reference (Red—Feeder 1, Black—Feeder 2, Blue—Feeder 3, Purple—Feeder 4, Orange—Feeder 5). Nodes where photovoltaic systems are connected are shown in green. The substation transformer is showing the nominal ratio without the off-load tap changer settings.

**TABLE 1** Consumers and photovoltaic systems connected to the secondary substation low voltage network.

Feeder	Phase	Single-phase		Three-phase	
		Consumers	PV	Consumers	PV
1	A	10	4	9	3
	B	12	4		
	C	19	2		
2	A	12	7	1	-
	B	15	6		
	C	9	5		
3	A	16	4	3	1
	B	25	7		
	C	17	2		
4	A	5	2	1	1
	B	12	3		
	C	13	4		
5	A	1	-	-	-
	B	13	4		
	C	13	1		

### 2.1 | Limitations

There is currently no data available for any deployed BESS in the Maltese LV distribution network. From a detailed analysis of the net-demand curves of all households over a year at the considered secondary substation, there is no clear evidence of any BESS being installed. However, the behaviour of any currently deployed BESS can be easily predicted since the local policies only promote the self-consumption of locally generated PV energy. Further information can be found in Sections 4.1.

The smart metres deployed in the residential settings do not record the reactive power data, and there is no information

about the power factor. However, by modelling the exact cable type as used by the utility, it is expected that the simulated node voltages perform close to those of the actual network. Each cable segment was modelled by a series of lumped parameter  $\pi$ -model transmission lines with the electrical specifications and lengths as provided by the DSO.

Most of the single-phase metres in households where PV systems were installed did not have any logs for the exported active power. Therefore, the relation between the PV generation and exported active power for this study had to be analysed and approximated for each individual consumer, based on the available substation master metre measurements.

### 3 | MALTESE LV NETWORK MODEL

The secondary substation was modelled in MATLAB/Simulink to perform a detailed analysis of the voltage profiles along the feeder. The simplified line diagram of the modelled LV network at the secondary substation is shown in Figure 1. The feeder nodes in which PV systems have been installed (either single phase or three phase) are shown in green. The PV generation curves were considered to be measured behind the metre of the customer premises, as per local utility regulations. The bus voltage magnitude  $|V_i|$  and its angle  $\delta_i$ , with respect to the reference voltage, can be determined from the active and reactive power of the loads and the distributed PV systems. Single-phase and three-phase load buses were implemented at the consumer locations. The distribution of the customers connected on each feeder and for each phase is shown in Table 1. This table also shows the subset of consumers having a residential PV system installed.

The 250 kVA, 11,000/400 V, 50 Hz, Dyn11 substation transformer with off-load tap changer supplies the five feeders from the secondary LV side, each with a different number of consumers connected to it. The primary side of the substation transformer acts as the slack bus (or swing bus) to balance the active power and reactive power. This bus acts as a reference to the simulation model and is the only known voltage at the start of the simulation. This means that during operation, the tap settings cannot be changed unless the transformer is de-energised. The off-load tap setting was set to  $-5\%$  such that the voltage levels at the end of the feeders have a suitable voltage level all year round, according to the limits defined in the Enemalta Network Code. This means that the effective turns ratio for the simulations was set to 10,450/400 V.

#### 3.1 | Distributed PV generation

The total installed PV capacity at the secondary substation is of 181 kWp (divided between 60 residential scale PV systems). The installed capacity consists of 161.88 kW single-phase systems distributed among 55 installations and 28.12 kW three-phase PV systems distributed among five installations. The nodes that contain a residential-scale PV system have been highlighted in Figure 1 for ease of reference. The histogram in

Figure 2 shows the peak power (kWp) ratings of the installed PV capacity grouped in bins of 0.5 kW. The single-phase PV systems range from 1.38 up to 4.38 kWp, while the three-phase PV systems range from 1.84 up to 10.8 kWp.

#### 3.2 | Analysis of the net-demand and selection of case scenario

An analysis of the substation net-demand characteristics over the considered year reveals that the highest magnitude of reverse power flow occurred on 12th March 2021. This day was selected as the case study for the analysis carried out in the following sections. The hourly net-demand and PV curve for this day are shown in Figure 3. The substation net-demand was determined from the simulations of the substation model carried out with the measured net-demand values obtained from the 192 consumer metres. The total PV generation curve was estimated by adding the measurements from all the 60 PV metres. Positive active power values for the net-demand represent the power consumed by the loads connected to that substation, while negative active power values represent the reverse power flow due to the local PV generation. The net-demand duck curve characteristic shows that oversupply occurs during the middle of the day since this coincides with the peak of PV generation. A negative net-demand occurs from 8.30 AM to 3.45 PM that reaches a peak of  $-109.7$  MW

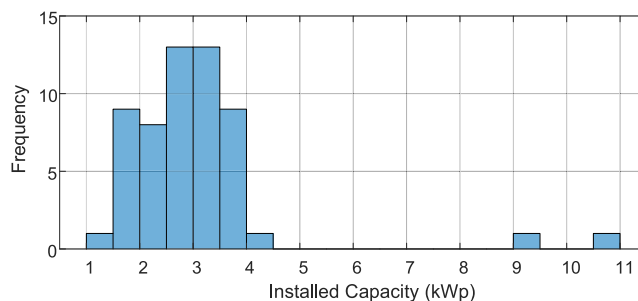


FIGURE 2 Histogram summarising the kWp ratings of the installed photovoltaic capacity grouped in bins of 0.5 kW.

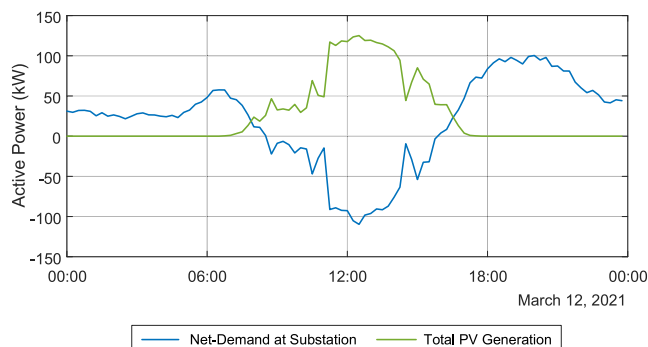


FIGURE 3 Net-demand characteristic and photovoltaic generation curve for the secondary substation during a high reverse power flow case scenario.

at 12.30 PM. This coincides with the instance of the daily maxima for PV generation having a value of 125.1 kW.

An analysis of the net-demand profiles for the 60 prosumers shows that in the majority of cases (approx. 65%), local PV generation exceeds the demand starting from 7.45 AM. However, in 25% of the prosumer households, the generation exceeds the electricity demand even earlier at 7 AM. From 9.45 AM onwards, all of the prosumer households have a negative net demand (i.e., are injecting the excess generation in the grid). Due to the different net demand characteristics, the electricity demand exceeds the local PV generation between 4.30 PM and 5.30 PM. However, in two of the prosumer households, the electricity demand exceeds the PV generation between 2 PM and 3 PM.

One should note that this study was performed during the COVID-19 pandemic. The COVID-19 pandemic has affected every aspect of life including the operation of the utility grid due to changes in the energy usage patterns of residential, commercial and public entities. According to a study published by the Malta National Statistics Office, the total electricity supplied in 2020 amounted to 2496.4 GWh which is a decrease of 5.4% when compared to the previous year [22]. The electricity demand during this period is expected to show a reduction from services and industry due to the lock-downs, while the residential electricity demand should show an increase.

### 3.3 | Transformer primary voltage profile

The nominal voltages of the national distribution system network defined in the Enemalta network code comply with standard MSA EN 50160:2010. The range tolerance for the LV network is 230 V  $\pm$ 10% (phase to neutral) and 400 V  $\pm$ 10% (phase to phase) under a steady state and normal operating conditions. To comply with MSA EN 50160:2010, the LV range tolerances should be satisfied during each period of 1 week, 95% of the 10 min mean r.m.s. At the 11 kV side of the substation transformer, the voltage range tolerance is of 11 kV  $\pm$ 5% (phase to phase).

The 24-h voltage profile at the primary windings of the transformer depends on the active and reactive power flows in the 11 kV network. Measurements of the actual voltage profiles at the substation were not available; however, the maximum and minimum phase voltages during the week at the substation were recorded at 248 and 232 V, respectively. The times when these voltages have occurred are also unknown. The voltage at the primary windings of the transformer was then estimated to vary between 1.03 pu (at the peak of the PV generation) and 0.95 pu (during the evening peak demand), respectively. The shape of the voltage profile was determined from a previous study performed by the authors on a section of the Maltese 11 kV network [23]. Figure 4 shows the estimated primary voltage profile over the considered 24 h at the substation transformer. This 24-h voltage profile was used as an input to all simulations that are described in the following sections.

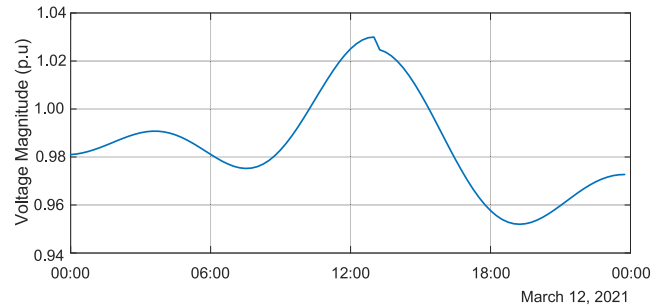


**FIGURE 4** Substation transformer per unit of the primary voltage profile.

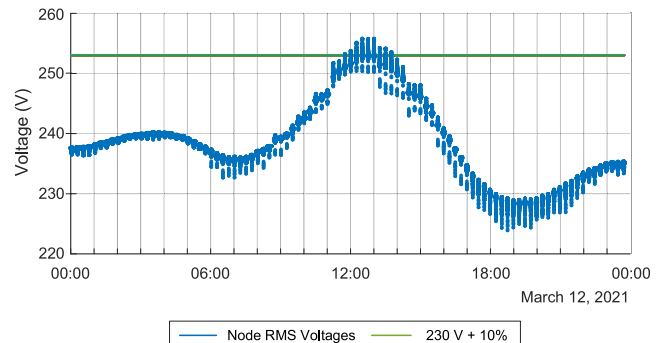


**FIGURE 5** Swarm plot of the node phase voltages in all five feeders at 15-min intervals throughout the day. The green line represents the 230 V +10% maximum limit (line-to-neutral). Each point is a resultant phase voltage at one of the nodes in the low voltage network.

### 3.4 | LV network node voltages for the present scenario

Figure 5 shows the phase (line-to-neutral) voltages of all the nodes present in the five feeders at 15-min intervals throughout the day. From the figure, one can observe that there are over-voltage events due to the reverse power flow between 11:45 AM and 2:00 PM. This corresponds to the period where solar PV generation reached a maximum. Violations of the 230 V +10% maximum limit were observed on all five feeders with the most severe occurring on feeder 3. All nodes in the feeder exceeded the maximum voltage threshold, while a maximum voltage of 255.8 V was observed at 1 PM on phase B at node 128.

The minimum voltage in the network of 223.8 V occurs in feeder 5 at phase C of node 176 at 6.45 PM, during the evening peak demand. Even though feeder 5 has the lowest number of nodes when compared with the other feeders, it is effectively the furthest node from the substation where a consumer is connected (at 621.85 m). Coincidentally, the consumer also has the highest electricity consumption for the day at nearly 46 kWh.

## 4 | COORDINATED VERSUS UNCOORDINATED DISTRIBUTED BESSs

This paper compares the effectiveness of uncoordinated and coordinated self-consumption strategies for voltage regulation purposes using the residential-scale BESSs. The first strategy

models the present Maltese scenario based on PV self-consumption that has no coordination among the storage units. The second strategy consists of a proposed improved tariff system for coordinated self-consumption using the behind-the-metre BESSs that could benefit both the consumer and the utility. It is being assumed that the change in the tariff system does not affect the behaviour of the consumers (no modifications in the original net-demand profiles). This was done to enable a direct comparison of the coordinated and uncoordinated scenarios, with the only variable being the utilisation of the distributed behind-the-metre BESSs.

#### 4.1 | Uncoordinated BESS operation: self-consumption

Behind-the-metre BESSs in Malta are mainly being deployed in the form of hybrid PV inverters (PV + batteries). The main aim of these units is to maximise PV self-consumption [24], as (1) the billing rates described in Section 5.4 are considerably higher than the presently available FiT of 0.105 €/kWh (for 20 years) for subsidised installations and 0.085 €/kWh for systems that have reached the end of-the contract; (2) there are no additional incentives for the integration of storage in the LV network (such as time-of-use rates). Prosumers can consume the electricity generated by the PV systems at the time it is produced while exporting any excess generation to the grid. Any electricity imported from the utility is charged at the applicable electricity tariffs as described in Table 1.

The uncoordinated BESS operation consists of a load-following mode in which the exchange of active power with the grid (import/export) is minimised within the constraints imposed by the battery SoC. The load-following operation aims to increase the level of self-consumption of the consumer by charging the BESS from the excess PV energy to offset the electricity demand during periods where the demand exceeds the local generation. The primary objective in this mode is to consume most of the energy generated by the distributed PV systems locally, reducing the need to import/export energy from/to the grid. This can be expressed mathematically as follows:

$$p_t^{\text{load}} = \min(p_t^{\text{PV}}, p_t^{\text{Demand}}) \quad (1)$$

where  $p_t^{\text{load}}$  is the electricity demand of the prosumer at time  $t$ ;  $p_t^{\text{Demand}}$  is the total load demand of the respective prosumer, and  $p_t^{\text{PV}}$  is the distributed PV generation by the respective prosumer. The power balance equation at the PCC of each prosumer, at time  $t$ , can be defined as follows:

$$p_t^{\text{grid}} = p_t^{\text{netload}} + p_t^{\text{charge,BESS}} - p_t^{\text{discharge,BESS}} \quad (2)$$

where  $p_t^{\text{grid}}$  is the power from/to the grid;  $p_t^{\text{netload}} = p_t^{\text{Demand}} - p_t^{\text{PV}}$  is the net-demand of the respective consumer, and  $p_t^{\text{charge,BESS}}$ ,  $p_t^{\text{discharge,BESS}}$  are the power charged and discharged by the BESS, respectively.

- 1) The BESS SoC was constrained to within the range between an  $\text{SoC}_t^{\text{min,BESS}}$  of 15% and an  $\text{SoC}_t^{\text{max,BESS}}$  of 100% to prolong the lifetime, that is,  $\text{SoC}_t^{\text{min,bess}} \leq \text{SoC}_t^{\text{actual,BESS}} \leq \text{SoC}_t^{\text{max,BESS}}$ , where  $\text{SoC}_t^{\text{actual,BESS}}$  is the actual battery SoC at any time of the day.
- 2) The useable energy capacity of the BESS was constrained to that within the range defined by the SoC constraints, that is,  $E_t^{\text{min,BESS}} \leq E_t^{\text{actual,BESS}} \leq E_t^{\text{max,BESS}}$ , where  $E_t^{\text{actual,BESS}}$  is the available battery energy at any time of the day.
- 3) The maximum discharge power  $P_t^{\text{discharge,BESS}}$  was limited to a maximum value,  $P_{\text{MAX}}^{\text{discharge,BESS}}$ , of 1C:  $P_t^{\text{discharge,BESS}} \leq P_{\text{MAX}}^{\text{discharge,BESS}}$ .
- 4) The maximum charging power  $P_t^{\text{charge,BESS}}$  was limited to a maximum value,  $P_{\text{MAX}}^{\text{charge,BESS}}$ , of 1C:  $P_t^{\text{charge,BESS}} \leq P_{\text{MAX}}^{\text{charge,BESS}}$ .
- 5) To maximise self-consumption, the BESS should be charged when PV generation exceeds the load and discharged when PV generation is insufficient to meet the load:

Charging BESS:

$$P_t^{\text{charge,BESS}} = \max(0, P_t^{\text{PV}} - P_t^{\text{Demand}}) \quad (3)$$

Discharging BESS:

$$P_t^{\text{discharge,BESS}} = \max(0, P_t^{\text{Demand}} - P_t^{\text{PV}}) \quad (4)$$

- 6) The actual energy stored in the BESS,  $E_t^{\text{actual,BESS}}$ , is determined by adding the net energy of the BESS from the previous time step,  $E_{(t-1)}^{\text{actual,BESS}}$ , to the energy charged in the BESS,  $E_t^{\text{charge,BESS}}$  and subtracting the discharged energy,  $E_t^{\text{discharge,BESS}}$  during the present time step. The energy conservation equation of the BESS is defined by the following equation:

$$E_t^{\text{actual,BESS}} = E_{(t-1)}^{\text{actual,BESS}} + E_t^{\text{charge,BESS}} - E_t^{\text{discharge,BESS}} \quad (5)$$

In this context, the ability of the distributed BESSs to reduce network peaks (peak demand and peak reverse flow) depends on the following:

- With residential billing tariffs being independent of the peak demand, the battery discharge can occur at any time. The BESS could contribute to the reduction of the utility peak demand if the discharge operation coincides with the secondary substation peak demand.
- With flat FiTs, there are no incentives to charge the BESS during the high reverse power flow periods. Depending on the size of the BESS and PV system, the BESS can be fully charged before the peak reverse power flow occurs at the secondary substation.

- The useable capacity of the battery and the rated power of the inverter. These system properties define how well the battery system can follow the household net-demand curve during charging and discharging.
- While the load-following mode is a basic function of off-the-shelf hybrid PV inverters, the performance of retrofitted non-coordinated residential BESSs in load following applications might not be up to the same level.

## 4.2 | Coordinated BESS operation: dynamic FiT

This study analyses how the coordinated self-consumption with distributed BESSs through the deployment of time-varying FiTs can benefit both the utility and the consumer. Since the vast majority of Maltese households (about 99%) have installed smart metres that are able to capture interval data (15 or 30 min resolution), customers could already benefit from a time-varying FiT without any changes to the present infrastructure. Real-time pricing and time-of-use tariffs are two additional strategies that could be used by consumers to shift loads, thus benefiting from preferential rates and resulting in better financial savings. However, real-time pricing requires additional ICT solutions to inform consumers about dynamic tariffs/prices.

Time-varying FiTs can enable prosumers to maximise the revenues from exported energy through the deployment of BESSs. The selection of the FiT interval bands can reduce the magnitude of the reverse power flow during mid-day and also reduce the evening peak electricity demand. In this mode of operation, the following conditions were considered and defined:

- 1) The BESS SoC was constrained to within the range between an  $\text{SoC}_t^{\min, \text{BESS}}$  of 15% and an  $\text{SoC}_t^{\max, \text{BESS}}$  of 100% to prolong the lifetime.
- 2) The useable energy capacity of the BESS was constrained to  $E_t^{\min, \text{BESS}} \leq E_t^{\text{actual, BESS}} \leq E_t^{\max, \text{BESS}}$ .
- 3) The maximum discharge power  $P_t^{\text{discharge, BESS}}$  was limited to a maximum value  $P_{\text{MAX}}^{\text{discharge, BESS}}$ , of 1C:  $P_t^{\text{discharge, BESS}} \leq P_{\text{MAX}}^{\text{discharge, BESS}}$ . A constant discharge rate was assumed for the BESS during the peak hours period.
- 4) The maximum charging power  $P_t^{\text{charge, BESS}}$  was limited to a maximum value,  $P_{\text{MAX}}^{\text{charge, BESS}}$ , of 1C:  $P_t^{\text{charge, BESS}} \leq P_{\text{MAX}}^{\text{charge, BESS}}$ .
- 5) The actual energy stored in the BESS,  $E_t^{\text{actual, BESS}}$ , is determined by adding the net energy of the BESS from the previous time step,  $E_{(t-1)}^{\text{actual, BESS}}$ , to the energy charged in the BESS,  $E_t^{\text{charge, BESS}}$ , and subtracting the discharged energy,  $E_t^{\text{discharge, BESS}}$  during the present time step. The energy conservation equation of the BESS is defined by the following equation:

$$E_t^{\text{actual, BESS}} = E_{(t-1)}^{\text{actual, BESS}} + E_t^{\text{charge, BESS}} - E_t^{\text{discharge, BESS}} \quad (6)$$

In this scenario, the ability of the distributed BESSs to reduce network peaks depends on the following:

- Having a high FiT during electricity peak demand hours which encourages BESS charged by excess PV generation to contribute to the reduction of the utility peak demand. This can be mathematically expressed as follows:

$$P_t^{\text{grid}} = \max\left(0, P_t^{\text{load}} - P_t^{\text{charge, BESS}} + P_t^{\text{discharge, BESS}}\right) \quad (7)$$

- Having a low FiT during periods of high PV generation to encourage PV owners to charge their BESS, minimising exports and thus contributing to the reduction of the reverse peak power flow. This can be mathematically expressed as follows:

$$P_t^{\text{grid}} = \min\left(P_t^{\text{load}} - P_t^{\text{charge, BESS}} + P_t^{\text{discharge, BESS}}, P_t^{\text{Demand}} - P_t^{\text{PV}}\right) \quad (8)$$

- The useable capacity of the battery and the rated power of the inverter.

The design strategies to determine minimum time-varying FiT rates are beyond the scope of this study. A time-varying FiT that is independent from the market price can offer guaranteed payments during specific times of the day over the period of the contract. While acknowledging that other strategies can be used to define the rates, the time-varying FiT proposed in Table 2 shall be used to highlight how prosumers with BESS can financially benefit from these tariffs. These time-varying bands were designed from the average annual electricity net-demand characteristic for the considered secondary substation. For Band B (11 AM to 4 PM), the rate was defined to be equal to the proxy for the local electricity market price for the year 2022. For Band C (4–10 PM), the rate was set at the maximum (non-subsidised) FiT currently available for the residential market. The rate for Band A (10 PM to 11 AM) was set at 96% of the subsidised flat FiT. The two flat tariffs in Table 2 are two actual FiTs presently used in Malta as described in an earlier section.

## 5 | LV NETWORK SIMULATION RESULTS

### 5.1 | Analysis of the net-demand with BESSs

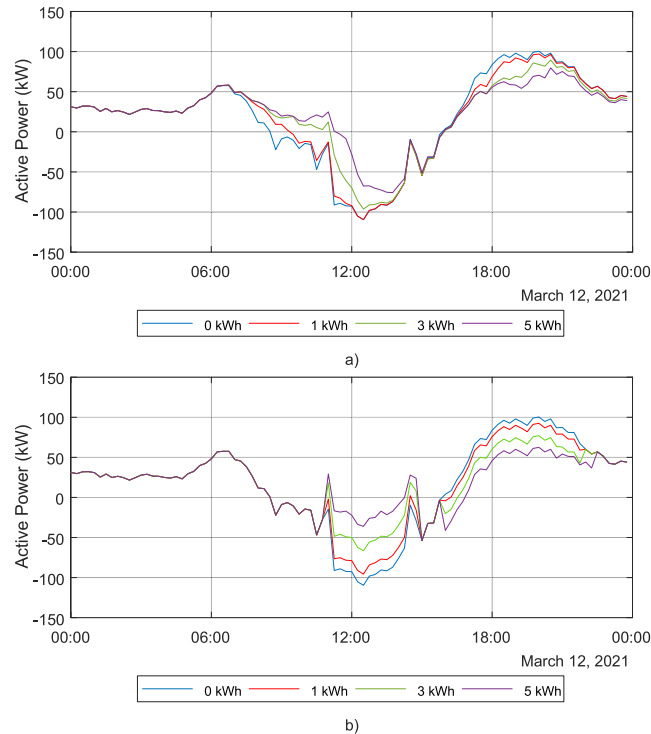
The hourly net-demand characteristics with different sizings of uncoordinated BESSs are shown in Figure 6a. The figure shows that BESSs affect the duck curve characteristic, reducing the reverse peak to -75.8 MW (30.9% change from the



**TABLE 2** Time-varying FiT versus flat FiT for prosumers with BESS.

Flat FiT (€/kWh)		Time-varying FiT (€/kWh)		
Subsidised	End of contract	Band A	Band B	Band C
0.105	0.0885	0.101	0.0885	0.15

Abbreviations: BESS, battery energy storage system; FiT, feed-in tariff.

**FIGURE 6** Net-demand characteristic for the secondary substation during a high reverse power flow case scenario. (a) With Uncoordinated BESSs. (b) With Coordinated BESS. BESSs, battery energy storage systems.

original net-demand curve) for the 5 kWh BESSs. In this case, the peak net demand shifted to 13.45 PM with the negative net demand occurring from 11.15 AM to 3.45 PM. The evening peak demand was reduced by 20.6% to 79.7 MW from the original net-demand curve with the introduction of the 5 kWh BESSs. This shifted the peak demand from 8 pm in the original net-demand characteristic to 8.30 PM (with 5 kWh BESSs).

For the uncoordinated scenario, the BESS sizing together with the reverse power profile (due to excess PV generation) determines how quickly the SoC of the batteries increases from the starting value of 15% up to the full capacity (100% SoC). For example, when considering the 1 kWh BESS scenario, 55% of the deployed BESSs were already fully charged before 9.30 AM and 88% fully charged by 11 AM. On the other hand, for the 5 kWh BESSs, only 65% were fully charged by 12.30 PM. For the latter scenario, two prosumer BESS installations reached full capacity as early as 9.30 AM, while in 5 cases, the full capacity was not reached during this day due to underperforming PV systems.

The BESSs supply energy to the local network when the electricity demand exceeds the local PV generation. Due to the

individual prosumer net demand characteristics, 63% of the deployed BESSs were already fully discharged by 7 PM when considering the 1 kWh BESS scenario. On the other hand, only 33% of the 5 kWh BESS scenario were fully discharged by 9.30 PM, while the rest had available capacity at the end of the day. In the latter, this occurs as the BESSs only displace the consumption at the prosumer such that the additional battery capacity can be used to displace consumption during the early hours of the following day. Consequently, their ability to store surplus PV generation the following day can be reduced. These results confirm what was observed from the literature, that although there was a reduction in the total energy flowing back to the substation and used during the evening peak period, the impact of uncoordinated BESSs was far less pronounced.

The hourly net-demand characteristics with different sizings of coordinated BESSs are shown in Figure 6b. The duck curve characteristics show that BESSs achieve an improved reduction of the reverse power flow when compared with the uncoordinated BESSs. The minimum peak reverse power flow of  $-50$  MW (54.4% change from the original net-demand curve) was obtained for the 5 kWh BESSs at 3.00 PM. With 3 kWh BESSs, the change in the peak reverse power flow was of 39.4%, showing that the coordinated operation achieves better performance with lower values of installed BESS capacity. The evening peak demand was reduced by 37.7% to 62.5 MW from the original net-demand curve with the introduction of the 5 kWh BESSs. With 3 kWh BESSs, the reduction in the peak demand was of 23%, showing that the even for peak shaving applications, the coordinated operation achieves better performance with lower values of installed BESS capacity.

For the coordinated scenario, the BESS sizing together with the reverse power profile (due to excess PV generation) determines the maximum charging rate of the BESS, while respecting the maximum charging current limit. The SoC of the batteries increases from the starting value of 15% up to the full capacity (100% SoC) or the maximum available capacity. The BESSs supply energy to the local network at a constant rate over the Band 3 time period such that the BESSs are fully discharged by the end of Band 3. For BESSs greater than and equal to 3 kWh, the BESSs not only displace the consumption at the prosumer households during the Band 3 period but can also inject more power contributing to reducing further the substation peak demand. These results confirm that the coordinated operation of BESSs under a self-consumption first scenario can achieve significantly better impact with a lower installed capacity.

## 5.2 | LV network node voltages with uncoordinated BESS

Figure 7 shows the phase voltages of all the nodes from the five feeders at 15-min intervals throughout the day with uncoordinated BESSs. Due to the effects in the reverse power flow characteristics described in the previous section, one can observe that the occurrence of overvoltage events reduces

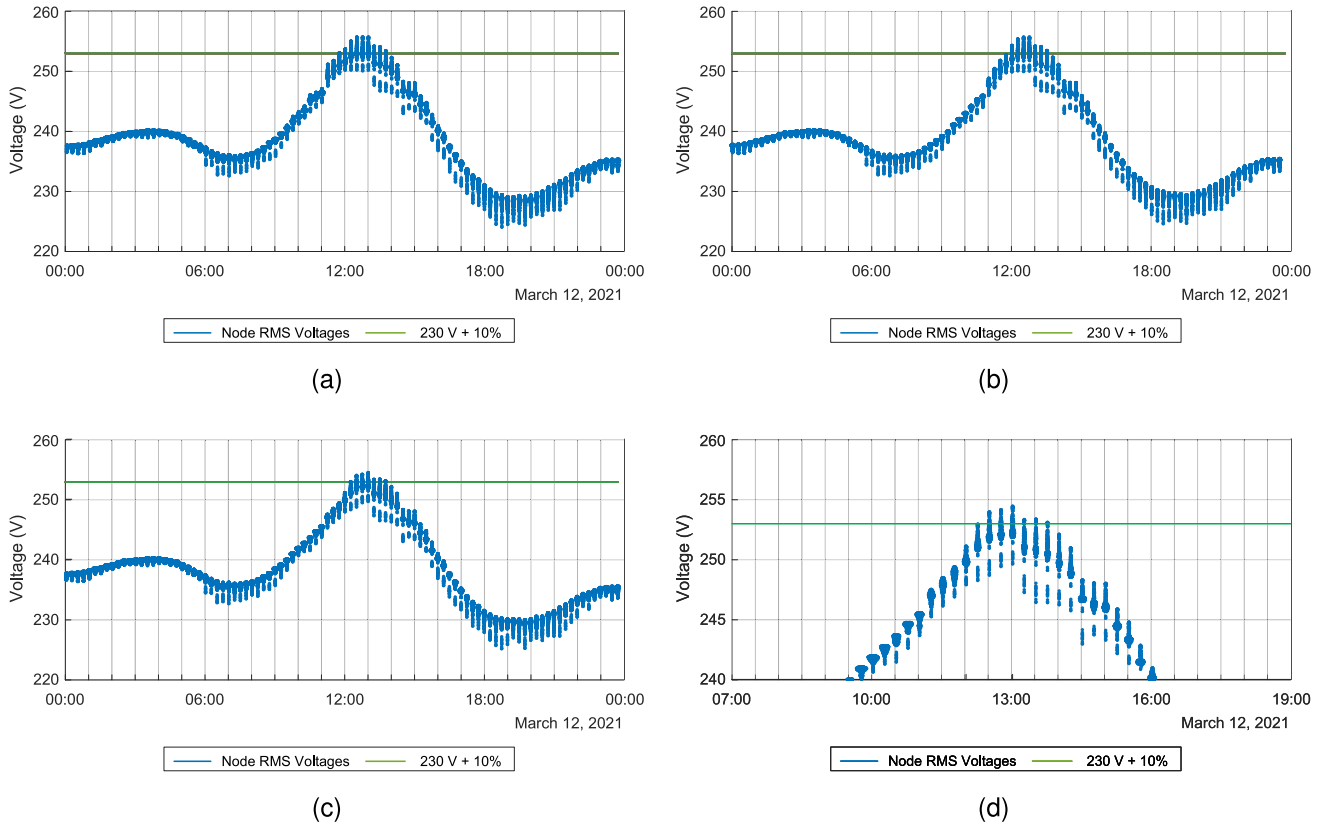


**FIGURE 7** Swarm plot of the node phase voltages in all five feeders at 15-min intervals throughout the day with uncoordinated BESSs. The green line represents the 230 V +10% maximum limit (line-to-neutral). Each point is a resultant phase voltage at one of the nodes in the low voltage network. (a) 1 kWh BESS. (b) 3 kWh BESS. (c) 5 kWh BESS. Part (d) is a zoomed view of the results in (c) around the maximum voltage limit. BESSs, battery energy storage systems.

between 11:45 AM and 2:00 PM as the size of the BESSs increases. In the scenarios with the 1 kWh and 3 kWh BESSs, the magnitude of the reverse power flow was not significantly affected by the uncoordinated BESS integration. Violations of the 230 V +10% maximum limit were observed on all five feeders with the most severe voltage magnitudes still occurring on feeder 3 with all nodes in the feeder exceeding the maximum voltage threshold. With the 5 kWh BESSs, there was a reduction in the magnitude and duration of the reverse power flow that resulted in overvoltage events occurring only in Feeders 1 and 3 between 12:30 AM and 1:45 PM. In this case, the maximum voltage of 254.5 V was observed at 1 PM on phase B at node 128 (change of  $-0.5\%$ ). Due to the reduction in consumption during the peak demand, the minimum network voltage increased to 225.08 V (change of  $+0.57\%$ ) with the 5 kWh BESSs in node 176 at 6.45 PM (phase C).

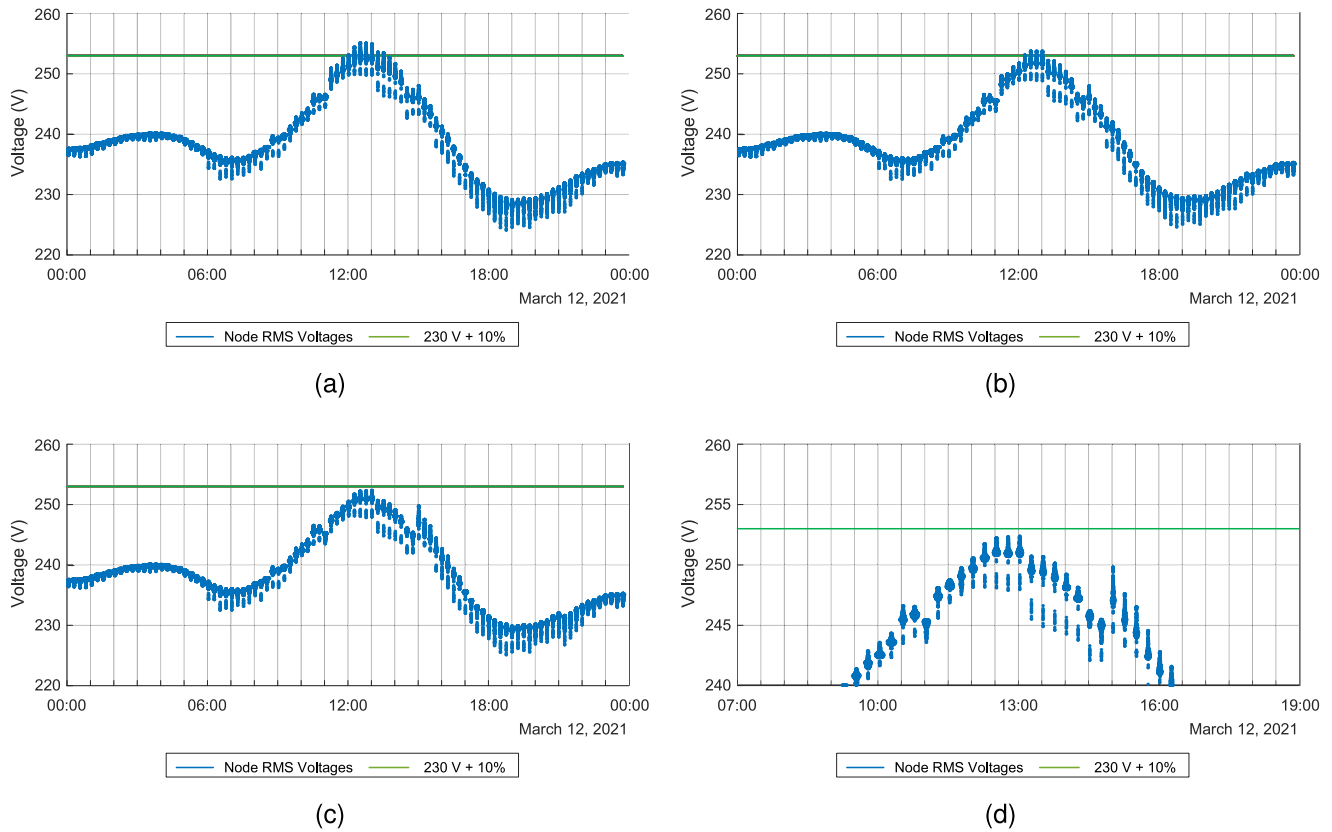
### 5.3 | LV network node voltages with coordinated BESS

Figure 8 shows the phase voltages of all the nodes present in the five feeders at 15-min intervals throughout the day with uncoordinated BESSs. One can observe that the occurrence of overvoltage events reduces during mid-day as the size of the BESSs increases with the coordinated storage. In the scenarios

with the 1 kWh and 3 kWh BESSs, the magnitude of the reverse power flow was already improved when compared with the uncoordinated BESS integration. Violations of the 230 V +10% maximum limit were observed only on feeder 1 and 3. The most severe voltage magnitudes are still occurring on feeder 3 with all nodes in the feeder exceeding the maximum voltage threshold. With the 5 kWh BESSs, there was a reduction in the magnitude and duration of the reverse power flow that resulted in no overvoltage events. In this case, the maximum voltage of 252.43 V was observed at 1 pm on phase B at node 128 (change of  $-1.32\%$ ). Due to the reduction in consumption during the peak demand, the minimum network voltage with the 5 kWh BESSs increased to 225.25 V (change of  $+0.65\%$ ) at node 176 at 6.45 PM (phase C).

### 5.4 | Prosumer net-billing analysis

In this section, the net-billing profitability of the prosumers with flat FiTs and a time-varying FiT shall be analysed for the considered case scenario. The billing rates in Table 3 are typically used to bill the electricity consumption on a pro-rata basis (typically bi-monthly) [25]. In this study, the billing rates were applied on a pro-rata basis for the day of interest, while discounts due to low annual cumulative consumption were not be considered. The net-billing profitability for the prosumers



**FIGURE 8** Swarm plot of the node phase voltages in all five feeders at 15-min intervals throughout the day with coordinated BESSs. The green line represents the 230 V +10% maximum limit (line to neutral). Each point is a resultant phase voltage at one of the nodes in the low voltage (LV) network. (a) 1 kWh BESS. (b) 3 kWh BESS. (c) 5 kWh BESS. Part (d) is a zoomed view of the results in (c) around the maximum voltage limit. BESSs, battery energy storage systems.

**TABLE 3** Residential electricity consumption rates [25].

Bands	Cumulative consumption kWh	Consumption tariff (inc. 5% VAT) €
Band 1	0–2000	0.1047
Band 2	2001–6000	0.1298
Band 3	6001–10,000	0.1607
Band 4	10001–20,000	0.3420
Band 5	>20,000	0.6076

in a self-consumption scenario with flat FiTs is shown in Figure 9. Self-consumption without storage resulted in the highest median profits for the end-of-contract FiT and subsidised FiT at €0.29 and €0.43, respectively. This scenario is presently the better choice for prosumers as the BESS roundtrip efficiency reduces the energy injection into the grid, resulting in reduced profits. The median profits with the 5 kWh BESSs reduced to €0.23 and €0.31 for the end-of-contract FiT and subsidised FiT, respectively. Prosumers thus need suitable incentives in order to deploy BESSs, especially to provide additional benefits to the grid.

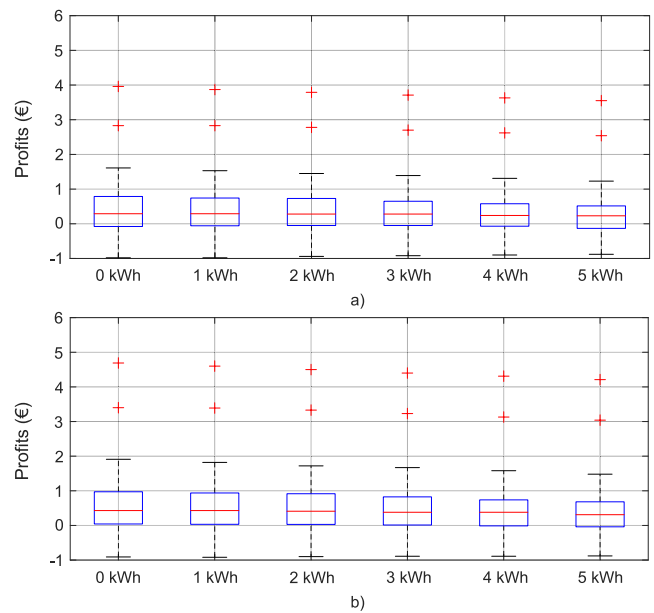


**FIGURE 9** Profitability for the prosumers in a self-consumption scenario with uncoordinated battery energy storage systems BESSs. (a) End-of-Contract feed-in tariff (FiT). (b) Subsidised FiT.

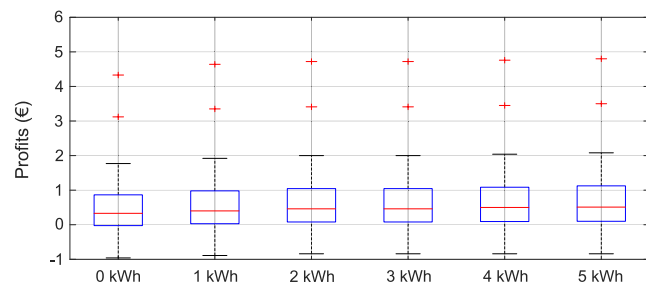


**FIGURE 10** Profitability for the prosumers in a self-consumption scenario with coordinated battery energy storage systems through the proposed time-varying FiT.

The net-billing profitability for the prosumers in a self-consumption scenario with time-varying FiT is shown in Figure 10. The introduction of the time-varying FiT transforms the downward trend of the net-billing profits to an upward trend against the increasing values of storage capacity. Self-consumption without storage now resulted in the lowest median profit at €0.33, nearly at the average of the two flat FiT strategies. The median profit with the 5 kWh BESSs increased to €0.51 without any changes to the consumption patterns. Further reduction of the electricity demand during the peak period could give rise to higher net-billing profits.

## 6 | CONCLUSION

This paper considered the integration of behind-the-metre BESSs in the Maltese LV distribution network. Strategies that aim towards maximising the self-consumption of the prosumers with both PV and BESSs were evaluated to verify the prosumer profitability as well as the benefit to the utility. Simulations have shown that the uncoordinated introduction of BESSs provides marginal benefits to the utility. Reduction of the power flows during periods of high PV generation as well as during the evening peak demands and can limit the overload of the cables and substation transformer. However, reductions that coincide with the peak reverse and evening power at the substation are purely coincidental due to the individual prosumer net demand characteristics. Time-varying FiTs were observed to provide benefits to both the prosumers and utilities without having the BESSs directly managed by the DSO. As the prosumers use the BESSs to shift their PV generation in order to maximise profitability, the design of the dynamic FiT bands can reduce the reverse peak power flow as well as the evening peak demand. Simulation results have shown that with the 5 kWh BESSs, there was a reduction in the magnitude and duration of the reverse power flow that resulted in no overvoltage events in all five feeders of the modelled substation. With the 5 kWh BESSs, there was a reduction in the magnitude and duration of the reverse power flow that resulted in no overvoltage events in all five feeders of the modelled substation. However, there was still stored capacity available within a few of the BESS that was left unused due to the discharging objectives defined for the BESS. In the context of the renewable energy communities outlined in this paper, this opens up the possibility of exploring other

applications. Specifically, there is the potential for BESSs to provide peer-to-peer services, thereby allowing both consumers and prosumers to buy and sell excess energy directly to each other within the community. However, a framework or platform must be defined to facilitate these transactions, including defining contracts and agreements between users and the owners of the BESS systems. This approach can promote energy sharing, optimise resource utilisation, and even potentially reduce costs for those involved. However, it is important to consider regulatory and technical aspects when implementing such a system, as well as ensuring that the primary objectives of the BESS are not compromised. This in turn can further improve the profitability of the BESS owners in addition to the aid of the FiT.

## AUTHOR CONTRIBUTIONS

**Alexander Micallef:** Conceptualisation; formal analysis; funding acquisition; investigation; methodology; project administration; resources; software; validation; visualisation; writing – original draft. **Cyril Spiteri Staines:** Conceptualisation; formal analysis; funding acquisition; investigation; methodology; project administration; validation; writing – review & editing. **John Licari:** Conceptualisation; formal analysis; investigation; methodology; validation; writing – review & editing.

## ACKNOWLEDGEMENTS

This research was financed by the Energy and Water Agency under the National Strategy for Research and Innovation in Energy and Water (2021–2030), grant agreement reference number ESTELLE EWA 110/20/2/001-C. The authors would like to acknowledge Enemalta for providing the data required to conduct this study.

## CONFLICT OF INTEREST STATEMENT

No conflict of interest to disclose.

## DATA AVAILABILITY STATEMENT

Data sharing is not applicable to this article as no new data were created or analysed in this study.

## ORCID

Alexander Micallef  <https://orcid.org/0000-0002-9497-5604>

## REFERENCES

- European Union: European Commission: 2022 Country Report Malta. Accompanying the document Recommendation for a COUNCIL RECOMMENDATION on the 2022 National Reform Programme of Malta and delivering a Council opinion on the 2022 Stability Programme of Malta, SWD(2022) 620 final (2022). [Online]. [https://ec.europa.eu/info/system/files/2022-european-semester-country-report-malta\\_en.pdf](https://ec.europa.eu/info/system/files/2022-european-semester-country-report-malta_en.pdf). Accessed 11 July 2022
- Regional, Geospatial, Energy and Transport Statistics Unit: Renewable Energy from Photovoltaic Panels (Pvs): 2021. National Statistics Office Malta, Tech. Rep. (2022). [Online]. [https://nso.gov.mt/en/News\\_Releases/Documents/2022/06/News2022\\_106.pdf](https://nso.gov.mt/en/News_Releases/Documents/2022/06/News2022_106.pdf). Accessed 11 July 2022
- Stecca, M., et al.: A comprehensive review of the integration of battery energy storage systems into distribution networks. *IEEE Open J. Ind.*

- Electron. Soc. 1(1) (2020). 1–1. <https://doi.org/10.1109/ojies.2020.2981832>
4. Martín, S., Pérez-Ruiz, J., López-Pérez, P.: Model to evaluate the system-wide impact of residential and commercial photovoltaic and storage units intended for self-consumption. *IET Renew. Power Gener.* 13(12), 2111–2122 (2019). <https://doi.org/10.1049/iet-rpg.2019.0228>
  5. Schram, W.L., Lampropoulos, I., van Sark, W.G.: Photovoltaic systems coupled with batteries that are optimally sized for household self-consumption: assessment of peak shaving potential. *Appl. Energy* 223, 69–81, (2018)
  6. Martínez, N., Tabares, A., Franco, J.F.: Generation of alternative battery allocation proposals in distribution systems by the optimization of different economic metrics within a mathematical model. *Energies* 14(6), 1726 (2021). <https://doi.org/10.3390/en14061726>
  7. Ordóñez, Á., et al.: Net-metering and net-billing in photovoltaic self-consumption: the cases of Ecuador and Spain. *Sustain. Energy Technol. Assessments*, 53, 102434 (2022). <https://doi.org/10.1016/j.seta.2022.102434>
  8. Ahmed, M., et al.: Effects of household battery systems on LV residential feeder voltage management. *IEEE Trans. Power Deliv.* 8977(c) (2022)
  9. Elbatawy, S., Morsi, W.: Integration of prosumers with battery storage and electric vehicles via transactive energy. *IEEE Trans. Power Deliv.* 37(1), 383–394 (2022). <https://doi.org/10.1109/tpwr.2021.3060922>
  10. Pena-Bello, A., et al.: Balancing DSO interests and PV system economics with alternative tariffs. *Energy Pol.* 183, 113828 (2023). <https://doi.org/10.1016/j.enpol.2023.113828>
  11. Saez, R., et al.: Techno-economic analysis of residential rooftop photovoltaics in Spain. *Renew. Sustain. Energy Rev.* 188, 113788 (2023). <https://doi.org/10.1016/j.rser.2023.113788>
  12. Parandeh, K., Bagheri, A., Jadid, S.: Optimal day-ahead dynamic pricing of grid-connected residential renewable energy resources under different metering mechanisms. *J. Mod. Power Syst. Clean Energy* 11(1), 168–178 (2023). <https://doi.org/10.35833/MPCE.2022.000440>
  13. Etchebehere, V.S., Marangon Lima, J.W.: Locational tariff structure for radial network fixed costs in a DER context. *IEEE Access* 10, 597–607 (2022). <https://doi.org/10.1109/ACCESS.2021.3137092>
  14. Zeraati, M., Hamedani Golshan, M.E., Guerrero, J.M.: Distributed control of battery energy storage systems for voltage regulation in distribution networks with high PV penetration. *IEEE Trans. Smart Grid* 9(4), 3582–3593 (2018). <https://doi.org/10.1109/tsg.2016.2636217>
  15. Wang, Y., et al.: Coordinated control of distributed energy-storage systems for voltage regulation in distribution networks. *IEEE Trans. Power Deliv.* 31(3), 1132–1141 (2016). <https://doi.org/10.1109/tpwr.2015.2462723>
  16. Hashemi, S., Østergaard, J.: Efficient control of energy storage for increasing the PV hosting capacity of LV grids. *IEEE Trans. Smart Grid* 9(3), 2295–2303 (2018)
  17. Wang, L., et al.: Coordination of multiple energy storage units in a low-voltage distribution network. *IEEE Trans. Smart Grid* 6(6), 2906–2918 (2015). <https://doi.org/10.1109/tsg.2015.2452579>
  18. Zarrilli, D., et al.: Energy storage operation for voltage control in distribution networks: a receding horizon approach. *IEEE Trans. Control Syst. Technol.* 26(2), 599–609 (2018). <https://doi.org/10.1109/tcst.2017.2692719>
  19. Deeba, S.R., et al.: A customer centric approach to the use of residential batteries for distribution network support. *IEEE Trans. Smart Grid* 10(5), 5449–5457 (2018). <https://doi.org/10.1109/tsg.2018.2883061>
  20. Procopiou, A.T., et al.: Adaptive decentralized control of residential storage in pv-rich mv-lv networks. *IEEE Trans. Power Syst.* 34(3), 2378–2389 (2019). <https://doi.org/10.1109/tpwrs.2018.2889843>
  21. Wang, S., et al.: Deep reinforcement scheduling of energy storage systems for real-time voltage regulation in unbalanced LV Networks with high PV penetration. *IEEE Trans. Sustain. Energy* 12(4), 2342–2352 (2021). <https://doi.org/10.1109/tste.2021.3092961>
  22. Regional, Geospatial, Energy and Transport Statistics Unit: Electricity Supply: 2016–2020. National Statistics Office Malta, Tech. Rep. (2021). [Online]. Available: [https://nso.gov.mt/en/News\\_Releases/Documents/2021/10/News2021\\_181.pdf](https://nso.gov.mt/en/News_Releases/Documents/2021/10/News2021_181.pdf). Accessed 11 July 2022
  23. Micallef, A., Spiteri Staines, C., Cassar, A.: Utility-scale storage integration in the Maltese medium-voltage distribution network. *Energies* 15(8), 2724 (2022). [Online]. <https://doi.org/10.3390/en15082724>
  24. Energy and Water Agency: Malta's 2030 National Energy and Climate Plan. Tech. Rep. (2020). [Online]. [https://www.energywateragency.gov.mt/wp-content/uploads/2021/10/MT-NECP-FINAL-2020-10-05\\_Corrigendum.pdf](https://www.energywateragency.gov.mt/wp-content/uploads/2021/10/MT-NECP-FINAL-2020-10-05_Corrigendum.pdf). Accessed 11 July 2022
  25. Laws of Malta: Electricity Supply Regulations. Government Gazette of Malta (2022)

**How to cite this article:** Micallef, A., Spiteri-Staines, C., Licari, J.: Voltage regulation in low voltage distribution networks with unbalanced penetrations of photovoltaics and battery storage systems. *IET Smart Grid*. 1–13 (2024). <https://doi.org/10.1049/stg2.12155>